

Optical properties of riverine dissolved organic matter and influence of precipitation – a case study

I. S. DONTU, C. L. POPA*, D. SAVASTRU, E. M. CARSTEA

National Institute of Research and Development for Optoelectronics - INOE 2000, 077125, str. Atomiștilor nr 409, Măgurele, Romania

The study aimed to determine the optical characteristics of dissolved organic matter (DOM) from two rivers with different pollution sources, using fluorescence spectroscopy and spectrophotometry, two highly sensitive and selective optoelectronic methods. Results showed that the release of wastewater effluent in Ciorogarla River changed the optical properties of riverine DOM and its relationship with standard parameters. It was also found that Sabar River samples presented high DOM concentrations and an accumulation of autochthonous matter towards mid-autumn. Although the study was performed on specific rivers, the knowledge that was obtained could be used as reference for other aquatic systems.

(Received February 28, 2024; accepted April 8, 2024)

Keywords: Rivers, Fluorescence spectroscopy, Dissolved organic matter, Surface runoff

1. Introduction

Rivers are dynamic systems that can substantially impact ecosystem processes, by transforming and carrying dissolved organic matter, nutrients and pollutants within the river and beyond [1]. Dissolved organic matter (DOM) is a complex mixture of compounds that originates from allochthonous or autochthonous sources [2]. DOM contributes to the carbon budget in aquatic systems, influences food webs, reduces ultraviolet radiation entering the water column, and affects biogeochemical processes and transport of pollutants across the system [1,3-6]. A fraction of DOM absorbs ultraviolet and visible light, and is referred to as chromophoric organic matter [2], while a small fraction of it also emits light after absorption, and is referred to as fluorescent organic matter. Chromophoric and fluorescent DOM are susceptible to changes in composition and function from alterations of hydrologic conditions, pollution events, land use and precipitation events [1]. Thus, it is highly important to understand the properties of DOM in various environmental conditions and multiple sources of pollution. However, there is limited understanding of the changes in chromophoric and fluorescent riverine DOM caused by agricultural and wastewater effluents and a high flow tributary.

Fluorescence spectroscopy and spectrophotometry are optoelectronic techniques capable of characterising aquatic dissolved organic matter with high sensitivity and selectivity [7]. Absorption is a precondition of fluorescence, and when a molecule absorbs radiation its energy increases, corresponding to the energy of an absorbed photon [8]. Fluorescence occurs when a molecule in an excited electronic state returns to the ground state by emitting a photon, with a lower energy compared to absorption [8].

Fluorescence spectroscopy uses emission and excitation spectra. An emission fluorescence spectrum is generated by maintaining a constant excitation wavelength, while varying the emission wavelength within a preestablished interval. This process gives rise to an intensity graph depending on the emission wavelength. It evidences the manner in which a sample responds when it is excited with a certain radiation wavelength, thus revealing the wavelengths for which fluorescence occurs. On the other hand, an excitation fluorescence spectrum is obtained by maintaining the emission wavelength constant, while varying the excitation wavelength. This approach enables the identification of the wavelengths that can be absorbed by the sample in order to fluoresce at a certain emission wavelength.

The aim of this study was to determine the optical characteristics of DOM from two rivers with different pollution sources, upstream and downstream of their confluence. In addition, the study aimed to establish a relationship between chromophoric and fluorescent DOM, and precipitation.

2. Experimental

2.1. Study Area and sampling

Samples were collected from five locations along Ciorogarla and Sabar rivers from the proximity of Măgurele, (N45°06', E26°01') which is situated near the capital of Romania, Bucharest city. The sampling frequency was bi-monthly, from January to December 2023. Two samples were collected upstream the confluence of the rivers and one sample downstream the confluence, from Sabar River (Fig. 1). Ciorogarla River has a length of 57 km and a catchment of 149 km². The

river is surrounded mainly by residential and agricultural areas, and collects surface runoff, untreated sewage and treated wastewater effluents from Magurele city. Ciorogarla MARS and Sabar MARS collection points (points 1,2 in Fig. 1) are located near MARS building (Magurele center for Atmosphere and Radiation Studies). Ciorogarla MARS point is downstream of a newly opened wastewater treatment plant and upstream of the Magurele city wastewater treatment plant (P.E. 14000). The Ciorogarla Alunis sampling point (point 3 in Fig. 1) is located downstream Magurele wastewater treatment plant.

Sabar River has a length of 174 km and stretches over 1,346 km². It collects agricultural and domestic wastewater.

The samples were collected in plastic bottles, which were pre-cleaned with a 20% RBS solution and thoroughly rinsed with distilled water to remove any contaminants potentially present in the bottles. All samples were filtered with 0.8 µm and 0.45 µm PVDF filters, which were pre-rinsed with distilled water. All measurements were made within 24 h from sample collection.

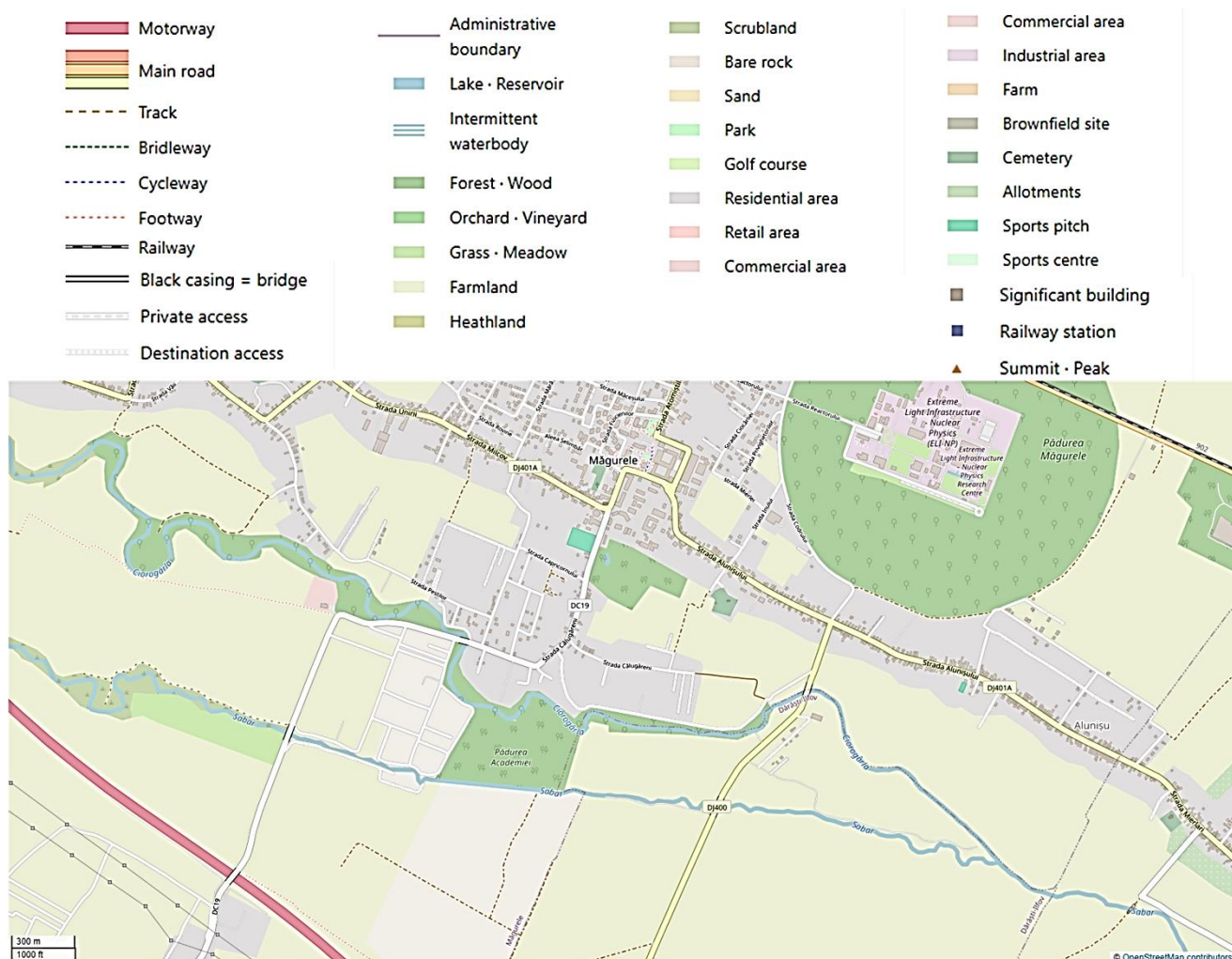


Fig. 1. Sampling points along Ciorogarla and Sabar Rivers: (1) Ciorogarla MARS, (2) Sabar MARS, (3) Ciorogarla Alunis, (4) Sabar Alunis, (5) Sabar Jilava. Blue stars indicate the location of the wastewater treatment plants, while the red drop indicates the location of the meteorological station. Map made with OpenStreet Map (color online)

2.2. Methods

2.2.1. Ancillary measurements

The following water quality parameters have been measured: pH, conductivity, turbidity, total/dissolved organic carbon (TOC), phosphate, nitrate, nitrite and total dissolved solids (TDS). The Hanna Instruments HI 255 combined meter was used to measure pH, conductivity, turbidity and TDS. For measuring TOC, phosphate, nitrate

and nitrite, the PF-12Plus photometer and testing kits from Macherey-Nagel were used. Precipitation data were collected from a meteorological station located near the sampling points [9].

2.2.2. Absorption and fluorescence measurements

Absorption spectra were recorded using a Thermo Fisher Scientific NanoDrop OneC spectrophotometer.

Spectral slopes of the regions 275-295 nm and 350-400 nm were calculated according to Helms et al. [2]. The spectral slopes and the ratio between the slopes of the two regions were found to be related to DOM molecular weight and to photochemically induced shifts in molecular weight [2].

Fluorescence spectra were recorded with a Jasco FP8200 spectrofluorimeter using the following parameters: excitation wavelength range 230-400 nm, step 2 nm; emission wavelength range 280-500 nm, step 2 nm; integration time 20 msec; bandwidth 5 nm for both excitation and emission; sensitivity medium; scan speed 1,000 nm/min. The spectrofluorimeter is equipped with a 150 W Xe lamp and a PMT detector. Raman values were recorded before each set of measurements to check the instrument stability. The average Raman value was 52.38 a.u. (SD = 0.44).

The peak-picking method, as described by Coble et al. [10] was used to process the fluorescence spectra. Five fluorescence peaks were identified: peak T ($\lambda_{\text{excitation}}/\lambda_{\text{emission}}$ 225 / 350 nm), peak B ($\lambda_{\text{excitation}}/\lambda_{\text{emission}}$ 225 / 305 nm), peak A ($\lambda_{\text{excitation}}/\lambda_{\text{emission}}$ 225 / 400-500 nm), peak M ($\lambda_{\text{excitation}}/\lambda_{\text{emission}}$ 310-320 / 380-420 nm) and peak C ($\lambda_{\text{excitation}}/\lambda_{\text{emission}}$ 300-350 / 400-500 nm) [10]. Generally, peaks T and B are associated with living or dead cellular matter and their byproducts. These peaks indicate the presence of microbial activity within aquatic systems, derived from natural and anthropogenic activities [11-12]. Peaks T and B are also present when the amino acid standards, tryptophan and tyrosine are found, and are thus generically names as tryptophan-like and tyrosine-like. Peaks A, C and M are associated with humic-like matter, from autochthonous (peak M) and allochthonous sources (peaks A and C) [13]. Peak A generally indicates terrestrial DOM, while peak M contains microbially reprocessed humic-like DOM [10] and peak C microbial by-products [14].

All the fluorescence data were blank corrected, but were not corrected for the inner filter effect or pH. According to Henderson et al [15], the inner filter effect is unlikely to occur at samples with absorption values of ≤ 0.05 , at a 1 cm pathlength cell and 340 nm wavelength, or at TOC values below 25 mg/L. Most of the samples (82%) presented absorption values within these limits. TOC varied between 2 mg/L and 29.5 mg/L, but only two samples presented values above 25 mg/L. The pH values varied between 7.19 and 8.11, and according to Osburn et al. [16], pH values within this range are unlikely to produce any changes in the fluorescence of DOM.

The following fluorescence indices have been calculated in order to provide a comprehensive view of the optical properties of DOM: the humification index (HIX), which indicates the degree of humification, the biological index (BIX), which shows the biological activity in water samples and the F_{450}/F_{500} index, which separates between sources of organic matter (autochthonous or allochthonous). These indices were calculated according to Huguet et al. [17] and McKnight et al. [18]. In addition, for the estimation of the predominance between

fluorescent components the ratio between fluorescence intensity peak T and peak C (T/C) was calculated.

2.2.3. Statistical analysis

The statistical analysis was performed using Python software and its libraries (Pandas for data manipulation and analysis, Matplotlib for creating plots and Pillow for image formatting), through ChatGPT v4.0, Data Analyst function. The results were checked for accuracy. The distribution of the data is significantly non-normal (Shapiro Wilk test, $W=0.30-0.98$, $p < 0.001$) and thus, Spearman's Rank correlation was determined between fluorescence data and standard water quality parameters, on 79 samples. Significance of differences between datasets was tested with Kruskal-Wallis and Nemenyi tests, using the Real Statistics tool.

3. Results and discussions

3.1. Ancillary measurements

The average values for the standard parameters are shown in Table 1. The pH values varied between 7.46 and 8.11 at Ciorogarla samples, and between 7.19 and 8.03 at Sabar samples. The pH did not vary significantly between seasons at any of the sampling points. Conductivity varied between 253 μS and 829 μS at Ciorogarla River. Slightly higher values were recorded for the sample downstream the wastewater treatment plant. Sabar River showed higher conductivity values upstream the confluence with Ciorogarla River, 745 – 1070 μS , compared to downstream sample, 303 – 769 μS , showing the dilution effect of Ciorogarla River on Sabar waters. In the case of Ciorogarla River, conductivity decreased slightly from the beginning of the year towards the end of summer, but increased abruptly in October due to higher precipitation during that period. On the contrary, Sabar MARS and Sabar Alunis locations, displayed a steady increase from January to December. The trend changed after the confluence of the two rivers and Sabar Jilava location showed a similar trend to Ciorogarla River.

TDS varied between 126 ppm and 415 ppm at Ciorogarla River, and at Sabar River between 152 ppm and 535 ppm. The influence of Ciorogarla River on Sabar River was also evident in the case of TDS, as concentrations in Sabar River decrease substantially after the confluence of the rivers. The same seasonal trend was observed at Ciorogarla River for total dissolved solids, as observed for conductivity.

Turbidity varied between 0.26 NTU and 94.60 NTU at Ciorogarla River, while at Sabar River it varied between 1.58 NTU and 96.20 NTU. Turbidity values increased at Sabar River after the confluence with Ciorogarla River. At samples Ciorogarla MARS, Ciorogarla Alunis and Sabar Jilava turbidity values decreased in the second half of the year, potentially from the impact of precipitation.

Sabar River had higher concentrations of TOC compared to Ciorogarla, in particular before the confluence point. The high TOC concentration in Sabar River potentially indicates pollution with domestic or agricultural wastewater. Sabar River also had higher concentrations of phosphates compared to Ciorogarla River. Phosphate concentrations varied between 0.20 mg/L and 0.90 mg/L at Ciorogarla River, while at Sabar River it varied between 0.20 mg/L and 3.30 mg/L. The high values at Sabar River were potentially caused by surface runoff

from agricultural areas, enriching the river with nutrients. This enrichment was also reflected in the higher concentrations of nitrate and nitrite in Sabar River compared to Ciorogarla River. Nitrate concentrations showed a steady increase from the beginning of the year towards the end, at Ciorogarla River (max. value 7.10 mg/L). On the contrary, at Sabar River, higher concentrations were observed in early spring and late autumn compared to the rest of the year (max. concentration 14 mg/L).

Table 1. Average values of standard water quality parameters for Ciorogarla and Sabar Rivers

Parameter	Ciorogarla MARS	Ciorogarla Alunis	Sabar MARS	Sabar Alunis	Sabar Jilava
pH	7.82	7.88	7.67	7.73	7.83
SD	0.17	0.15	0.25	0.20	0.14
CV	0.02	0.02	0.03	0.03	0.02
Median	7.87	7.94	7.70	7.76	7.83
EC (μ S)	385.93	445.18	894.19	908.53	474.11
SD	95.95	146.50	87.47	84.04	151.90
CV	0.25	0.33	0.10	0.09	0.32
Median	387.00	396.00	874.00	883.00	442.00
Turbidity (NTU)	21.95	22.01	17.45	14.76	22.77
SD	28.24	26.81	14.84	12.43	26.99
CV	1.29	1.22	0.85	0.84	1.18
Median	8.95	11.25	13.55	10.80	8.71
TOC (mg/L)	2.04	4.36	8.09	7.95	4.54
SD	0.11	6.25	8.44	9.17	5.66
CV	0.05	1.43	1.04	1.15	1.25
Median	2.00	2.00	4.65	4.50	2.00
PO ₄ (mg/L)	0.36	0.31	1.30	1.45	0.48
SD	0.26	0.18	0.59	0.80	0.27
CV	0.72	0.58	0.45	0.55	0.55
Median	0.20	0.30	1.25	1.40	0.40
NO ₃ (mg/L)	3.03	2.91	4.25	3.54	3.14
SD	1.89	1.76	4.18	3.62	1.64
CV	0.62	0.61	0.98	1.02	0.52
Median	2.10	2.15	1.85	1.80	2.75
NO ₂ (mg/L)	0.15	0.14	0.20	0.26	0.28
SD	0.17	0.15	0.19	0.22	0.19
CV	1.17	1.07	0.97	0.87	0.67
Median	0.06	0.07	0.10	0.16	0.27
TDS (ppm)	192.77	224.00	452.07	454.27	239.13
SD	49.65	75.64	40.21	42.18	78.27
CV	0.26	0.34	0.09	0.09	0.33
Median	195.00	195.00	437.00	441.00	228.00

SD – standard deviation; CV – coefficient of variation; EC – electrical conductivity; TOC – total organic carbon; TDS – total dissolved solids

3.2. Fluorescence and absorption measurements

3.2.1. Spatial and seasonal DOM variation at Ciorogarla River

Fluorescent components showed distinct behaviour compared to each other (Fig. 2). Peak B was significantly different ($p < 0.001$) from peaks T and A, but not from peaks C and M. In Ciorogarla River, peaks B, C and M may have the same autochthonous origin, related to

microbial reprocessing. These peaks displayed very little variation throughout the year, and no influence from precipitation or photodegradation during the summer. Peak A was significantly different ($p < 0.001$) from peaks B and C, but not from peaks T and M. Peaks A and M components followed the same trend along the year, potentially showing that peak M represents a mixture of allochthonous and autochthonous DOM sources. Nevertheless, a higher contribution of DOM from

terrestrial sources was observed, in Ciorogarla River, compared to freshly reprocessed microbial DOM.

Both locations from Ciorogarla River were dominated by peak T (Fig. 2). This dominance is also reflected by the ratio between peaks T and C. Peak T was significantly different ($p < 0.001$) from peak B, indicating a different source for these components. Peak T was also significantly different from peak C ($p < 0.01$), which shows that peak T components do not contribute to DOM reprocessing in this river. Particularly high peak T fluorescence was recorded, at Ciorogarla Alunis sample, in September 2023, along

with peak M. Peak T was 8 times and peak M 11 times more intense, during this sampling date compared to the other dates. This sampling date was preceded by the driest period of the year, with an average of 0.18 mm from the beginning of August to mid-September. The release of wastewater effluents dominated by microbial DOM, coupled with low water levels and high summer temperatures may have enhanced the microbial activity in Ciorogarla Alunis location. However, a localized pollution event with untreated sewage cannot be excluded as a potential source of high peak T.

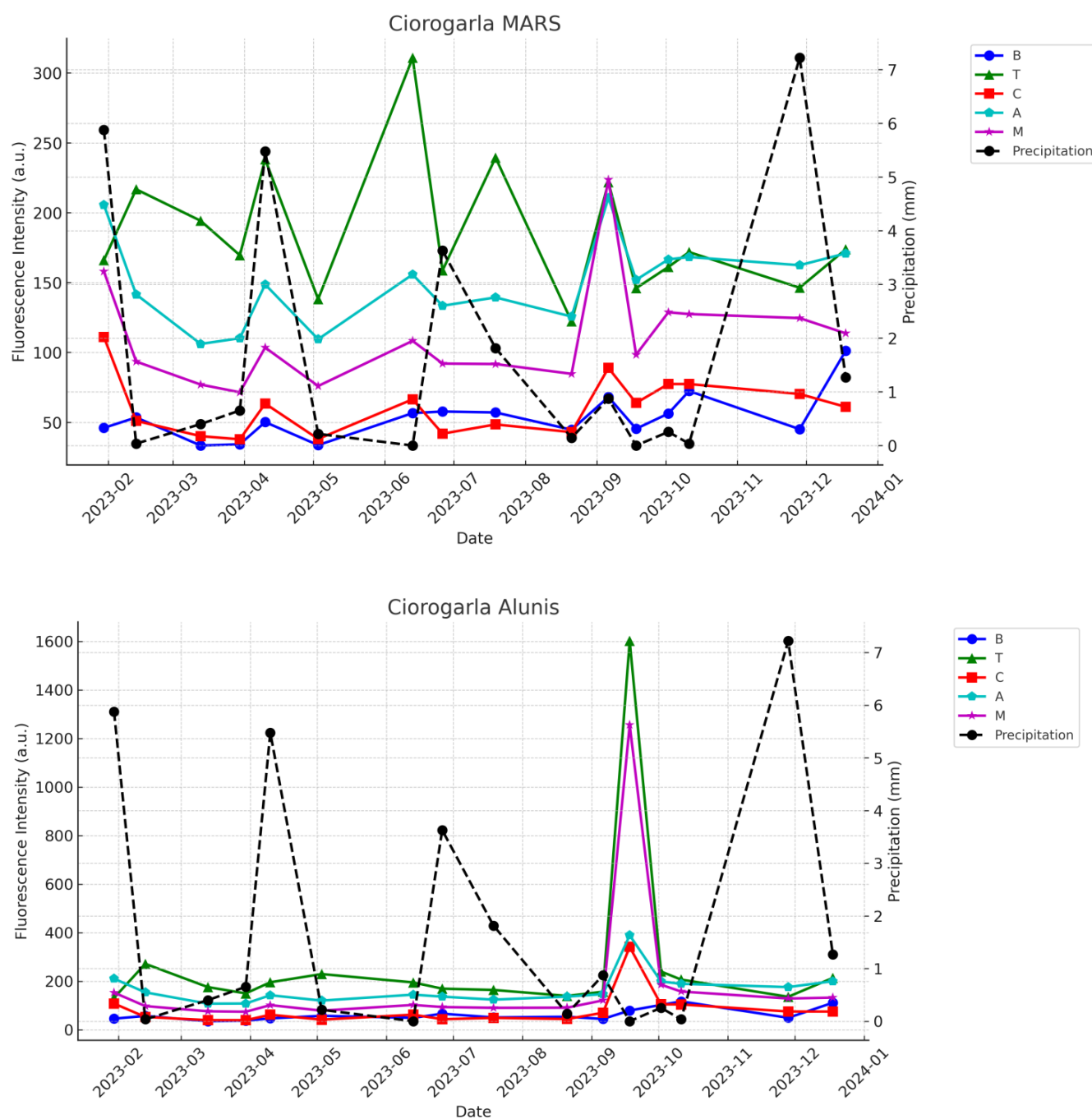


Fig. 2. Seasonal evolution of dissolved organic matter fluorescence from Ciorogarla River in relation to precipitation (one week average prior to sampling) (color online)

HIX and BIX indicators showed that the Ciorogarla MARS samples contained DOM with strong to intermediate autochthonous component and weak humic character. One exception was recorded in January 2023, when DOM was characterized by an important humic contribution and low autochthonous component. Potentially, snowmelt moved higher quantities of terrestrial DOM compared to rainfall. Contrary to HIX and BIX, F450/500 ranged between 1.20 and 1.37, for Ciorogarla MARS samples, and values close to 1.30 were associated, in previous studies, with terrestrial and soil derived DOM [18]. However, this indicator may not be relevant in comparing aquatic system with high spatial variability [17].

The slope ratio S_R is inversely related to molecular weight [2]. At Ciorogarla MARS samples, the S_R values showed that the molecular weight of DOM decreases from

the beginning of the year towards autumn and increases again towards winter (Fig. 3). Photobleaching, of high molecular weight peak C in particular, during summer and early autumn may be responsible for the decrease in molecular weight [2]. Snowmelt and rainfall may bring high molecular weight DOM from soil. A significant negative correlation was found between S_R and sampling day precipitation ($\rho = -0.77$, $p < 0.01$) and with one week average precipitation ($\rho = -0.64$, $p < 0.05$). No relationship was observed for spectral slopes. Also, no seasonal trend in spectral slopes or slope ratio was observed at Ciorogarla Alunis sample. The results showed that the release of wastewater effluents potentially changed the pattern of natural DOM in Ciorogarla River.

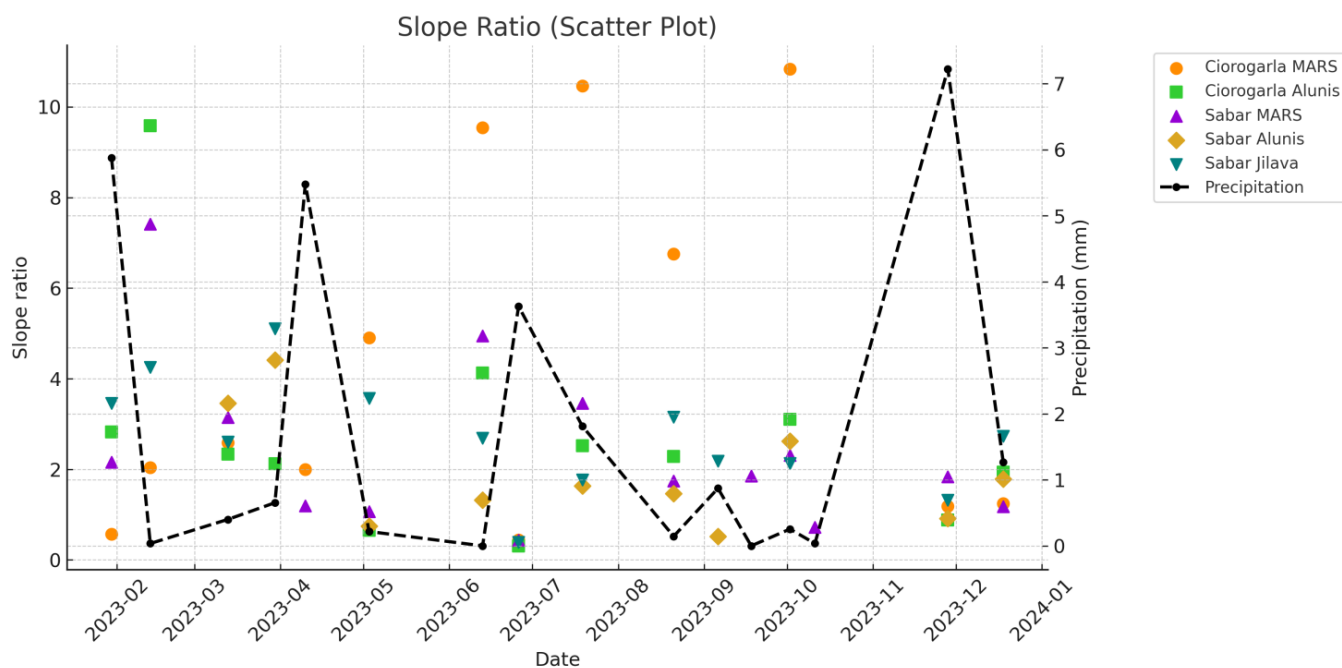


Fig. 3. Slope ratio ($S_{275-295}/S_{350-400}$) in relation to precipitation (average of one week prior to sampling) (color online)

Further analysis of the parameter relationships with fluorescence highlights the differences between the two sampling points and the impact of wastewater effluents. At Ciorogarla MARS samples, peaks A, C and M correlated significantly ($p < 0.05-0.01$) with nitrite, conductivity and TDS. The highest correlations were found between nitrite and peak C ($\rho = 0.83$, $p < 0.01$), peak A ($\rho = 0.85$, $p < 0.01$) and peak M ($\rho = 0.88$, $p < 0.01$). No correlation was found between peak T and standard parameters and only a low correlation of peak B with nitrite ($\rho = 0.54$, $p < 0.05$). The release of wastewater effluent decreased the correlation coefficients determined between nitrite and peak C ($\rho = 0.57$, $p < 0.05$), peak A ($\rho = 0.56$, $p < 0.05$)

and peak M ($\rho = 0.66$, $p < 0.01$). However, it increased the correlation between peak B and nitrite ($\rho = 0.61$, $p < 0.05$).

3.2.2. Spatial and seasonal DOM variation in Sabar River and influence of Ciorogarla River

At Sabar River MARS and Alunis samples, only peak B was significantly different from peak T ($p < 0.01$) and peak A ($p < 0.05$). At Sabar Jilava sample, apart from peak B being significantly different from peaks T and A ($p < 0.001$), peak T was significantly different from peak C ($p < 0.001$) and peak C was significantly different from peak A ($p < 0.001$). Peak T dominated at all Sabar samples (Fig.

4). The ratio between peaks T and C also indicated the dominance of the microbial-like fraction compared to humic-like. At Sabar MARS and Alunis samples, all peaks fluorescence intensity increased from mid-spring to mid-autumn and decreased abruptly with the rise in the quantity of precipitation (Fig. 4). However, no significant correlation was observed with precipitation. Longer monitoring periods, with large storm events, are needed to establish a clear relationship. The accumulation of DOM during spring and summer contradicts the findings of Shousha et al. [1], in particular in relation to peaks T and C, which are more prone to photodegradation. Here, there is potentially a major source of pollution from the upstream towns, which have seen rapid residential development in the past decade, ahead of wastewater treatment infrastructure development.

A clear distinction was observed between Sabar samples before and after the confluence with Ciorogarla. Firstly, the fluorescence peaks of Sabar MARS and Sabar Alunis were significantly different ($p < 0.001$) than Sabar Jilava, in terms of behaviour and intensity. For example, the fluorescence intensity of peak T was two- to four-fold higher at Sabar MARS and Alunis samples than Sabar Jilava. However, Sabar Jilava presents similar values to Ciorogarla samples, showing a clear impact of tributary river DOM on main river DOM characteristics. This is similar to the findings of Acharya et al. [19]. Secondly, at Sabar MARS and Alunis locations, peak M presented the highest intensities among humic-like peaks, whereas at Sabar Jilava samples, peak A dominated. This shows that the tributary changes the optical properties of DOM, bringing a high concentration of terrestrial matter, overlapping and diluting the microbially reprocessed DOM. It also shows that a large tributary can mask potential pollution events on the main river.

HIX and BIX revealed the strong autochthonous nature of DOM in Sabar River. The autochthonous character of DOM increased towards the end of the year at Sabar MARS and Alunis samples. At Sabar Jilava samples, HIX varied throughout the year, without an evident trend, due to the influence from Ciorogarla River DOM. However, BIX showed higher values towards the end of the year from a potentially combined contribution of microbial DOM accumulation in the upstream part of Sabar River and September pollution event that occurred in Ciorogarla River. The average values of F450/500 were slightly higher at Sabar MARS and Sabar Alunis (1.39) compared to Sabar Jilava (1.31). But, Sabar Jilava presented slightly higher F450/500 values compared to Ciorogarla samples (1.27). Although there are only slight differences between values, the F450/500 indicator was able to separate the mixed contribution of DOM from the tributary and main river.

As in the case of Ciorogarla samples, the slope ratio S_R , at Sabar samples, showed an increase in DOM molecular weight towards the end of the year (Fig. 3). This was potentially caused by photobleaching of labile high molecular weight DOM and an accumulation throughout the year of low molecular weight DOM. Longer monitoring periods are needed to determine if this is an yearly trend.

The difference between the two rivers is additionally highlighted by how DOM relates to phosphates and nitrates. Significant correlation was found between phosphates and all fluorescence peaks: peak B ($\rho = 0.85-0.87$, $p < 0.01$), peak T ($\rho = 0.78-0.87$, $p < 0.01$), peak C ($\rho = 0.84-0.88$, $p < 0.01$), peak A ($\rho = 0.84-0.88$, $p < 0.01$) and peak M ($\rho = 0.81-0.83$, $p < 0.01$). Since Sabar River crosses a large agricultural area (Fig. 1), a potential explanation for the level of phosphate and DOM may be the release of runoff with phosphate fertilisers. However, phosphate concentrations did not correlate with the quantity of precipitation. Nevertheless, all fluorescence peaks correlated negatively with nitrate and nitrite. In particular, highly significant negative correlations were found, at Sabar Alunis samples, between nitrate and peak B ($\rho = -0.71$, $p < 0.01$), peak T ($\rho = -0.70$, $p < 0.01$), peak C ($\rho = -0.72$, $p < 0.01$), peak A ($\rho = -0.72$, $p < 0.01$) and peak M ($\rho = -0.68$, $p < 0.01$). Here, phosphate also correlated negatively to nitrate ($\rho = -0.86$, $p < 0.01$). These results may indicate a legacy pollution with phosphates, which may be released through the process of denitrification together with organic carbon [20]. More studies are required to understand the source of these relationships. At Sabar Jilava location, downstream of the confluence with Ciorogarla River, the samples showed no significant correlation between fluorescent DOM and phosphates. Only a low correlation with peak A ($\rho = 0.51$, $p < 0.05$) was seen. Also, all fluorescence peaks correlated positively with nitrate and nitrite, which is contrary to the results found for the upstream samples. However, the correlation coefficients with nitrate were higher at Sabar Jilava than those found at Ciorogarla samples: peak B ($\rho = 0.71$, $p < 0.01$), peak C ($\rho = 0.76$, $p < 0.01$), peak A ($\rho = -0.74$, $p < 0.01$), peak M ($\rho = 0.78$, $p < 0.01$). The contribution of the tributary with DOM clearly changed the properties of the main river DOM.

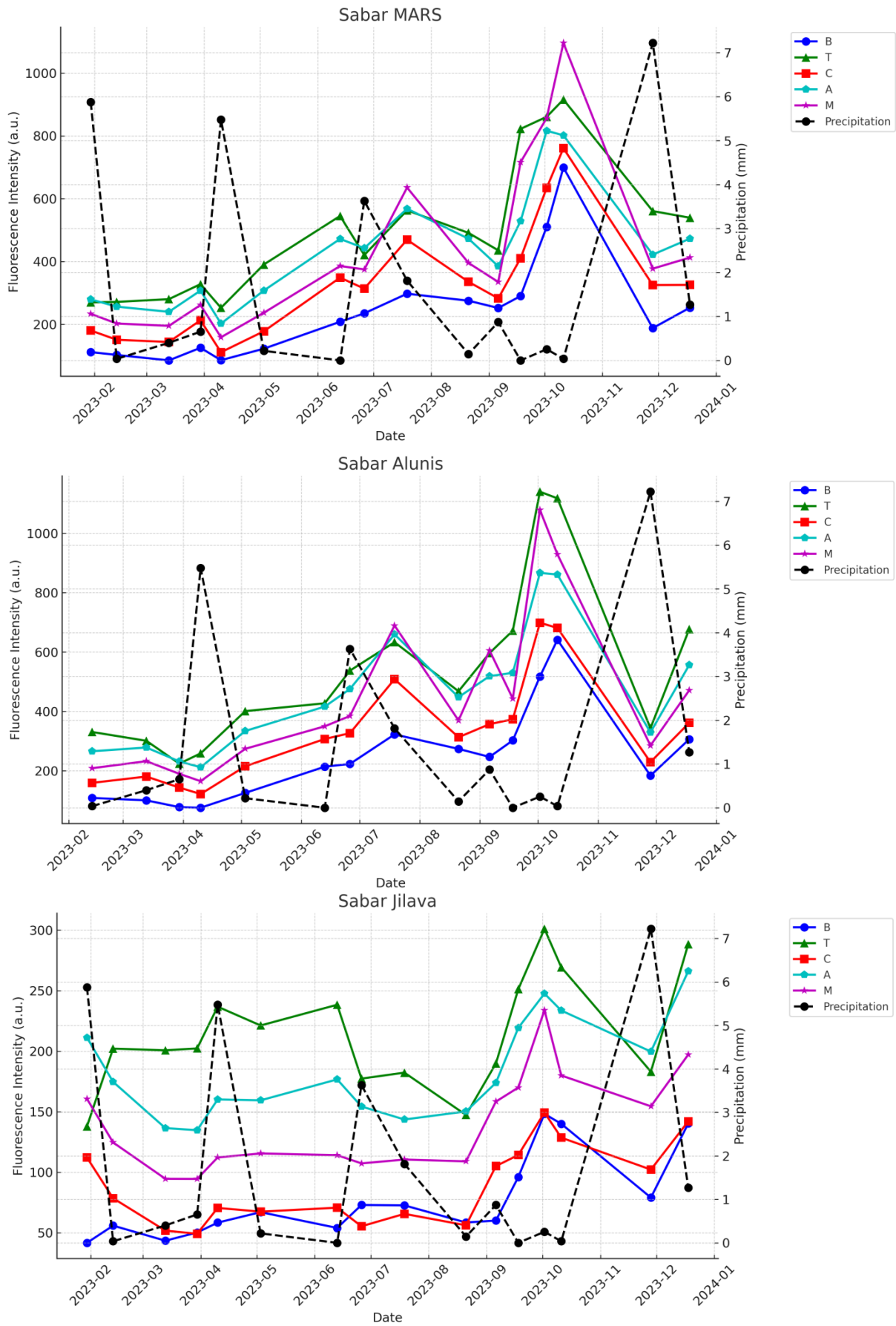


Fig. 4. Seasonal evolution of dissolved organic matter fluorescence from Sabar River in relation to precipitation (one week average prior to sampling) (color online)

4. Conclusions

The study showed that the release of wastewater effluent in Ciorogarla River did not significantly increase DOM concentration in the river. However, it changed the optical properties of riverine DOM and its relationship with standard parameters. It was also found that Sabar River samples presented high DOM concentrations and an accumulation of autochthonous matter towards mid-autumn. The large precipitation events from late autumn decreased the quantity of microbial DOM. However, longer monitoring periods, with large storm events, are needed to establish a clear relationship. The results also showed that a tributary can completely change the DOM character in the main river and even mask pollution sources. The slope ratio did not clearly distinguish between the different DOM characteristics of the two rivers. However, the absorption slope ratio showed an increase in DOM molecular weight towards the end of the year, at both rivers.

Acknowledgements

The authors acknowledge the support of the Romanian Ministry of European Investment and Projects, the Ministry of Research, Innovation and Digitalization, and CNCS – UEFISCDI, through the following projects: PN-III-P4-PCE-2021-0585 (Contract no. 78/2022); 18PFE/30.12.2021; Core Program OPTRONICA VII PN23 05 (11N/2023); 152/2016, SMIS 108109. Supplementary data are available at request.

References

- [1] S. Shousha, R. Maranger, J. F. Lapierre, *Biogeochemistry* **161**, 207 (2022).
- [2] J. P. Helms, A. Stubbins, J. D. Ritchie, E. C. Minor, D. J. Kieber, K. Mopper, *Limnol. Oceanogr.* **53**(5), 955 (2008).
- [3] D. P. Morris, B. R. Hargreaves, *Limnol. Oceanogr.* **42**(2), 239 (1997).
- [4] S. Baken, F. Degryse, L. Verheyen, R. Merck, E. Smolders, *Environ. Sci. Technol.* **45**(7), 2584 (2011).
- [5] P. Massicotte, J. J. Frenette, *Ecol. Appl.* **21**(7), 2600 (2011).
- [6] C. Fasching, C. Akotoye, M. Bazic, J. Fonville, D. Ionescu, A. Mathavarajah, L. Zoccarato, D. A. Walsh, H. P. Grossart, M. A. Xenopoulos, *Limnol. Oceanogr.* **65**(S1), 71 (2020).
- [7] C. L. Popa, I. S. Dontu, I. C. Ioja, G. O. Vanau, A. M. Popa, C. H. Gandescu, A. Stan, D. M. Cotorobai, D. Savastru, E. M. Carstea, *J. Optoelectron. Adv. M.* **25**(11-12), 554 (2023).
- [8] D. M. Reynolds, *The Principles of Fluorescence in Aquatic Organic Matter Fluorescence*, Cambridge University Press, New York, 3 (2014).
- [9] ISS-LPSM – IMGURE1 meteorological station, <https://www.wunderground.com/dashboard/pws/IMGURE1>.
- [10] P. G. Coble, R. G. M. Spencer, A. Baker, D. M. Reynolds, *Aquatic Organic Matter Fluorescence in Aquatic Organic Matter Fluorescence*, Cambridge University Press, New York, 75 (2014).
- [11] J. Bridgeman, A. Baker, C. Carliell-Marquet, E. Carstea, *Environ. Technol.* **34**(23), 3069 (2013).
- [12] H. Yu, Y. Song, R. Liu, H. Pan, L. Xiang, F. Qian, *Chemosphere* **113**, 79 (2014).
- [13] N. Hudson, A. Baker, D. Reynolds, *River Res. Appl.* **23**, 631 (2007).
- [14] B. G. Fox, R. M. S. Thorn, A. M. Anesio, T. Cox, J. W. Attridge, D. M. Reynolds, *Water* **11**, 1 (2018).
- [15] R. K. Henderson, A. Baker, K. R. Murphy, A. Hambly, R. M. Stuetz, S. J. Khan, *Wat. Res.* **43**, 863 (2009).
- [16] C. L. Osburn, R. del Vecchio, T. J. Boyd, *Physicochemical effects on dissolved organic matter fluorescence in natural waters in Aquatic Organic Matter Fluorescence*, Cambridge University Press, New York, 233 (2014).
- [17] A. Huguet, L. Vacher, S. Relexans, S. Saubusse, J. M. Froidefond, E. Parlanti, *Org. Geochem.* **40**(6), 706 (2009).
- [18] D. M. McKnight, E. W. Boyer, P. K. Westerhoff, P. T. Doran, T. Kulbe, D. T. Anderson, *Limnol. Oceanogr.* **46**(1), 38 (2001).
- [19] S. Acharya, A. Holland, G. Rees, A. Brooks, D. Coleman, C. Hepplewhite, S. Mika, N. Bond, E. Silvester, *Wat. Res.* **237**, 119975 (2023).
- [20] A. Musolff, B. Selle, O. Buttner, M. Opitz, J. Tittel, *Glob. Chang. Biol.* **23**(5), 1891 (2017).

*Corresponding author: cristina.popa@inoe.ro